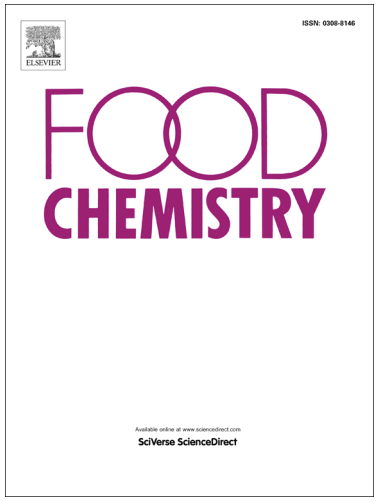

Covalent binding of food-derived blue pigment phycocyanobilin to bovine β-lactoglobulin under physiological conditions

Simeon Minic, Mirjana Radomirovic, Nina Savkovic, Milica Radibratovic, Jelena Mihailovic, Tamara Vasovic, Milan Nikolic, Milos Milcic, Dragana Stanic-Vucinic, Tanja Cirkovic Velickovic

PII: S0308-8146(18)31111-7
DOI: https://doi.org/10.1016/j.foodchem.2018.06.138
Reference: FOCH 23099

To appear in: *Food Chemistry*

Received Date: 5 March 2018
Revised Date: 6 June 2018
Accepted Date: 27 June 2018

Please cite this article as: Minic, S., Radomirovic, M., Savkovic, N., Radibratovic, M., Mihailovic, J., Vasovic, T., Nikolic, M., Milcic, M., Stanic-Vucinic, D., Velickovic, T.C., Covalent binding of food-derived blue pigment phycocyanobilin to bovine β-lactoglobulin under physiological conditions, *Food Chemistry* (2018), doi: https://doi.org/10.1016/j.foodchem.2018.06.138

Covalent binding of food-derived blue pigment phycocyanobilin to bovine β-lactoglobulin under physiological conditions

Simeon Minic[a], Mirjana Radomirovic[a], Nina Savkovic[a], Milica Radibratovic[b,c], Jelena Mihailovic[a], Tamara Vasovic[a], Milan Nikolic[a], Milos Milcic[c,d*], Dragana Stanic-Vucinic[a] and Tanja Cirkovic Velickovic[a,c,e*]

[a]Center of Excellence for Molecular Food Sciences & Department of Biochemistry, University of Belgrade - Faculty of Chemistry, Belgrade, Serbia

[b]Center for Chemistry - Institute of Chemistry, Technology and Metallurgy, University of Belgrade, Belgrade, Serbia

[c]Ghent University Global Campus, Yeonsu-gu, Incheon, South Korea

[d]Center for Computational Chemistry and Bioinformatics & Department of Inorganic Chemistry, University of Belgrade - Faculty of Chemistry, Belgrade, Serbia

[e]Faculty of Bioscience Engineering, Ghent University, Ghent, Belgium

*Corresponding authors at Ghent University Global Campus, Yeonsu-gu, Incheon, South Korea and University of Belgrade – Faculty of Chemistry, Belgrade, Serbia:

E-mail address: Tanja.Velickovic@ghent.ac.kr (TCV), tcirkov@chem.bg.ac.rs (TCV); mmilcic@chem.bg.ac.rs (MM).

Abstract

In this study, we investigated structural aspects of covalent binding of food derived blue pigment phycocyanobilin (PCB) to bovine β-lactoglobulin (BLG), major whey protein, by spectroscopic, electrophoretic, mass spectrometry and computational methods. At physiological pH (7.2), we found that covalent pigment binding *via* free cysteine residue is slow (k_a = 0.065 min^{-1}), of moderate affinity ($K_a = 4x10^4\ M^{-1}$), and stereo-selective. Binding also occurs at a broad pH range and under simulated gastrointestinal conditions. Adduct formation rises with pH, and in concentrated urea (k_a = 0.101 min^{-1}). The BLG-PCB adduct has slightly altered secondary and tertiary protein structure, and bound PCB has higher fluorescence and more stretched conformation than free chromophore. Combination of steered molecular dynamic for disulfide exchange, non-covalent and covalent docking, favours Cys119 residue in protein calyx as target for covalent BLG-PCB adduct formation. Our results suggest that this adduct can serve as delivery system of bioactive PCB.

Key words: β-lactoglobulin, Phycocyanobilin, Phycocyanin, Covalent, Binding, *Spirulina*, Fluorescence, Molecular Docking.

1. Introduction

Phycocyanobilin (PCB), a blue linear tetrapyrrole chromophore, is covalently attached to C-phycocyanin (C-PC), protein involved in light harvesting during photosynthesis in cyanobacteria species. C-PC is the major protein of *Spirulina*, microalgae with proven health promoting activities. Interestingly, dozens of *in vitro* and *in vivo* studies have shown significant antioxidant, anti-inflammatory, anticancer and immunomodulatory activities of C-PC (**Fernández-Rojas, Hernández-Juárez, & Pedraza-Chaverri, 2014**). In addition, recent preclinical evidence supports the application of C-PC and PCB as agents for promotion of neural tissue regeneration in multiple sclerosis and ischemic stroke (**Penton-Rol, Marin-Prida, & Falcon-Cama, 2018; Cervantes-Llanos, Lagumersindez-Denis, Marin-Prida, Pavon-Fuentes, Falcon-Cama, Piniella-Matamoros, et al., 2018**). PCB is mainly responsible for the health benefits of C-PC, mostly due to excellent antioxidant activities of tetrapyrrole pigment (**Zhou, Liu, Chen, Wang, Chen, Zhang, et al., 2005**). On the other hand, intensive blue colour, as well as high fluorescence intensity in VIS region, makes C-PC and PCB good candidates for applications in the food industry (as natural food colorants) (**Mysliwa-Kurdziel & Solymosi, 2017**; **Jespersen, Stromdahl, Olsen, & Skibsted, 2005**).

PCB is attached *via* a thioether bond to cysteine residues of apoproteins. Addition of PCB to C-PC is catalyzed by phycobiliprotein lyases. However, spontaneous attachment to apo-phycocyanin also occurs (**Scheer & Zhao, 2008**). Some studies assumed that phycobiliprotein lyases do not represent real enzymes, but they act more like chaperones, protecting chromophores from oxidation and enabling it to take proper conformation, adequate for energy

transfer during photosynthesis (**Scheer & Zhao, 2008**). Moreover, it is well-known that PCB can react with compounds bearing free SH groups, such as cysteine (**Bishop, Nagy, O'Connell, & Rapport, 1991**) and ethanethiol (**Klein & Rüdiger, 1979**). Therefore, it seems that PCB has capability for spontaneous attachment to any protein with (exposed) free cysteine residue(s).

Bovine β-lactoglobulin (BLG), the major whey protein of cow's milk, is one of the best studied proteins. It comprises about 50% of total whey proteins and 10% of whole cow's milk proteins (**Le Maux, Bouhallab, Giblin, Brodkorb, & Croguennec, 2014**). BLG belongs to lipocalin protein family, whose members have a widely diverse series of functions, including ligand binding. It is assumed that BLG's ability to bind and transport lipophilic compounds is a physiological reason for its high abundance in milk (**Kontopidis, Holt, & Sawyer, 2004**). BLG has at least two ligand binding sites, which in previous studies have been shown to simultaneously bind different ligands, such as retinol, fatty acids, cholesterol and phenol compounds (**Teng, Xu, & Wang, 2015**). BLG folds up into an 8 stranded, antiparallel β-barrel with a 3 turn α-helix on the outer surface and a 9 β-strand flanking the first strand (**Kontopidis, et al., 2004**). BLG has two intramolecular disulfide bonds and one free SH group (Cys121). One disulfide bond is formed between Cys66 and Cys160, while the second bond is formed between Cys106 and Cys119 (**Creamer, Bienvenue, Nilsson, Paulsson, van Wanroij, Lowe, et al., 2004**). The free SH group is responsible for polymerization properties of BLG due to the capability to form intermolecular disulfide bonds, as well as to promote disulfide exchange. BLG association and formation of aggregates depend on pH, temperature and ionic strength of protein solution (**Gottschalk, Nilsson, Roos, & Halle, 2003**).

Good solubility in a broad pH range, as well as numerous techno-functional properties (such as emulsion stabilization and gel formation), make BLG a suitable choice for use as an

additive in the food industry (**Singh, 2011**). It is well known that ligand binding by non-covalent interactions influences thermal and proteolytic stability of food proteins (**Celej, Montich, & Fidelio, 2003**). Binding of PCB to proteins could significantly change bioactivities, bioavailability and stability of both interacting partners, as previously shown for serum albumins (**Minic, Stanic-Vucinic, Radomirovic, Radibratovic, Milcic, Nikolic, et al., 2018; Minic, Milcic, Stanic-Vucinic, Radibratovic, Sotiroudis, Nikolic, et al., 2015; Radibratovic, Minic, Stanic-Vucinic, Nikolic, Milcic, & Cirkovic Velickovic, 2016**).

In this study, we characterized for the first time binding of food-derived blue pigment PCB to BLG. Binding affinity and kinetics were analyzed using fluorescence spectroscopy. SDS-PAGE and mass spectrometry (MS) have revealed covalent binding of PCB to cysteine residues, resulting in a fluorescently labeled BLG. We demonstrated covalent adduct formation also in the simulated gastrointestinal conditions. Effects of PCB binding on BLG's secondary and tertiary structures were studied by far-UV and near-UV CD spectroscopy. PCB conformational changes upon binding were examined by UV/VIS absorption and near-UV/VIS CD spectroscopy. Combination of steered molecular dynamic (SMD) simulation and docking showed target sites for non-covalent and covalent PCB binding to BLG.

2. Materials and methods

2.1. Materials

BLG was isolated and purified from raw cow's milk, as previously described (**Stojadinovic, Burazer, Ercili-Cura, Sancho, Buchert, Cirkovic Velickovic, et al., 2012**). BLG concentration was determined spectrophotometrically using the extinction coefficient of 17,600 $M^{-1}cm^{-1}$ at 278 nm (**Collini, D'Alfonso, & Baldini, 2000**). PCB was purified from

commercial Hawaiian *Spirulina pacifica* powder (Nutrex, USA) and then quantified from stock solutions in DMSO, as previously described (**Minic, et al., 2015**). C-PC was isolated and purified from the same source, as previously described (**Zhang & Chen, 1999**). All experiments were done in 20 mM sodium phosphate buffer, pH 7.2, except for pH dependence study and simulated gastro-intestinal conditions (see below). Final concentrations of DMSO in BLG-PCB mixtures did not exceed 5% (v/v). All other chemicals were of analytical reagent grade and Milli-Q water (Millipore, France) was used as a solvent.

2.2. Fluorescence measurements

All fluorescence measurements were performed using a FluoroMax®-4 spectrofluorometer (HORIBA Scientific, Japan) under thermostated conditions. BLG was serially diluted from 256 µM to 0.5 µM. Then, 4 µM PCB was mixed 1:1 (v/v) with protein dilutions or buffer. Obtained mixtures were incubated at 37°C for 2 hours. Upon incubation, fluorescence spectra were recorded between 600 and 700 nm at 37°C, with excitation wavelength of 580 nm, while excitation and emission slit widths were set to 5 nm. Emission of free PCB was subtracted from BLG-PCB complex fluorescence and apparent binding constant was calculated by fitting experimental data (at 640 nm) into equation (1) (**Keppler, Stuhldreier, Temps, & Schwarz, 2014**):

$$\Delta F = \frac{F_\infty \text{ x } [BLG]}{\frac{1}{K_a} + [BLG]} \quad (\mathbf{1})$$

where [BLG] is concentration of protein in µM, K_a is the apparent binding constant for BLG-PCB complex, F_∞ is fluorescence of BLG-PCB complex at infinite concentration of BLG, while ΔF was obtained by subtraction of free PCB fluorescence from BLG-PCB complex fluorescence.

Comparison of fluorescence spectra of PCB-amino acid mixtures and BLG-PCB complex were performed by incubation of PCB with cysteine, arginine, lysine, histidine or BLG in molar ratio 1:1 (20 µM each) for 2 hours at 37°C. Before measurements, each mixture was diluted 10 times. Fluorescence spectra were recorded as described above.

Kinetics of BLG-PCB complex formation was studied by recording pigment fluorescence upon BLG addition. Reaction was performed in the presence and absence of 7 M urea. BLG and PCB were mixed in 1:1 molar ratio (5 µM both) and fluorescence was being recorded during 2000 s at every 20 s. Excitation and emission wavelengths were of 580 and 640 nm, respectively, and slits were set to 5 nm. Fluorescence of free PCB was subtracted from BLG-PCB adduct fluorescence at each time point. Concentration of unbound PCB was calculated according to equation (2):

$$[\mathrm{PCB}] = 5 - 5 \times \frac{F_t - F_0}{F_\infty - F_0} \quad \textbf{(2)}$$

where F_t represents fluorescence of BLG-PCB complex at time t, F_0 and F_∞ are fluorescence at zero and infinite time, respectively, while 5 is the starting concentration of PCB in µM. Binding rate constant was calculated by fitting obtained results into first order kinetics using equation (3):

$$[\text{free PCB}] = 5 \times e^{-k \times t} \quad \textbf{(3)}$$

where [free PCB] represent concentration of unbound ligand, while *k* and t represent apparent binding rate constant and time, respectively.

Kinetics study of PCB binding to alkylated BLG was performed in the presence of 7 M urea, as described above. Alkylated BLG was obtained by incubation of 200 µM BLG with 100 mM iodoacetamide (IAA) in the same solution, during 1 hour at 37°C, with subsequent dialysis (during 24 hours at 4°C) against buffer.

2.3. CD measurements

All CD measurements were carried out on Jasco J-815 spectropolarimeter (Jasco, Japan) under thermostated conditions (at 37^{o}C). Before CD measurements all BLG samples were extensively dialyzed during 24 hours against buffer at 4^{o}C. Experimental details are given in Supplementary materials.

2.4. UV/VIS absorbance spectroscopy measurements

UV/VIS absorption spectra were recorded using a NanoDrop 2000c spectrophotometer (Thermo Scientific, USA). The measurements of 50 µM BLG and BLG-PCB complex after dialysis (Section 2.6.), as well as 50 µM free PCB, were made in the range of 300–750 nm at room temperature.

2.5. SDS-PAG electrophoresis

Formation of covalent adduct between BLG and PCB was observed after SDS polyacrylamide gel electrophoresis (SDS-PAGE), using the ability of PCB to complex Zn^{2+} ions and forms fluorescent product. BLG-PCB mixture (20 µM each), 20 µM free protein and 20 µM free pigment were incubated at 37^{o}C for 2 hours. SDS-PAGE was performed under standard non-reducing conditions on 16% PAA gel, followed by gels incubation in 1 M $ZnSO_4$ during 15 minutes. Fluorescence arising from PCB-Zn^{2+} complex was visualized under an UV lamp, while the gels were subsequently stained with Coomassie Brilliant Blue R-250 and gel images were scanned.

In order to compare the yield of the adduct formation in urea and buffer, BLG-PCB mixture (100 µM each), 100 µM free protein and 100 µM free PCB were incubated at 37^{o}C for 2

hours in the presence and absence of 7 M urea. After incubation, samples are diluted to 20 µM and subjected to SDS-PAGE, as previously described.

Dependence of BLG-PCB adduct formation on solution's pH was studied by incubation of equimolar BLG-PCB mixture (20 µM) in 50 mM phosphate-citrate buffer, varying pH from 2 to 9. Incubation was performed at 37^{o}C during 2 hours. Obtained samples are subjected to SDS-PAGE as previously described.

Inhibition of BLG-PCB adduct formation by IAA was electrophoretically analyzed as described above. 20 µM BLG in the absence and presence of 20, 200 and 2000 µM IAA were pre-incubated for 30 minutes at 37^{o}C, followed by addition of 20 µM PCB and subsequent incubation for 2 hours at the same temperature.

2.6. Preparation of BLG-PCB adduct at higher yield

PCB was being added to 200 µM BLG in four equal portions (after each 30 minutes at 37^{o}C) to obtain 300 µM final concentration of ligand with total incubation time of 2 hours, followed by extensive dialysis (about 24 hours) against buffer at 4^{o}C. In order to obtain higher yield of adduct, the dialyzed BLG was additionally enriched with PCB and again subjected to dialysis as previously described. The same procedure was applied to free BLG (control), except that instead of PCB, equivalent volumes of DMSO were mixed with protein.

2.7. Determination of BLG-PCB reaction yield

Two approaches were used in order to determine the yield of BLG-PCB adduct formation. The first one is based on determination of free SH groups in proteins by Ellman's reagent, 5,5'-dithio-bis(2-nitrobenzoic acid) (DTNB) (**Ellman & Lysko, 1979**).

The second approach is based on the use of whole pepsin digest of C-PC as standard, considering that the concentration of the chromophore in the digest is known (**Minic, Stanic-Vucinic, Mihailovic, Krstic, Nikolic, & Cirkovic Velickovic, 2016**). Experimental and calculation details for both approaches are given in Supplementary materials.

2.8. Detection of BLG-PCB adduct by mass spectrometry

BLG-PCB adduct was obtained by incubation of 200 μM BLG and 200 μM PCB, for 2 hours at 37^{o}C. Obtained adduct was diluted to 20 μM protein concentration by acetonitrile (MeCN) and formic acid (FA), so the final concentrations of MeCN and FA were 50% and 1%, respectively. BLG-PCB complex was subjected to high resolution tandem mass spectrometry using LTQ Orbitrap XL (Thermo Fisher Scientific Inc., USA) mass spectrometer as previously described (**Minic, et al., 2016**) with some modifications. Experimental details are given in Supplementary materials.

2.9. Computational methods

The crystal structure of BLG (ID: 3NQ3) was obtained from the Protein Data Bank (PDB). The details of the docking and SMD studies are presented in Supplementary material.

2.10. Reaction of BLG and PCB in simulated gastrointestinal conditions

Formation of BLG-PCB adduct was also studied in simulated gastro-intestinal conditions. Experimental conditions were the same as previously described (**Minekus, Alminger, Alvito, Ballance, Bohn, Bourlieu, et al., 2014**), except that addition of enzymes was omitted. Briefly, equimolar mixture of BLG and PCB (500 μM both) was mixed with simulated salivary fluid (SSF) at 1:1 ratio (v/v). After 2 minutes, the obtained mixture was mixed with simulated gastric

fluid (SGF) at 1:1 ratio (v/v). Incubation in SGF was being performed during 2 hours, followed by mixing with simulated intestinal fluid (SIF) at 1:1 ratio (v/v) and same incubation time (2 hours). At every stage, aliquots were taken for SDS-PAGE analysis (as described above), while the BLG concentration in each aliquot was adjusted to 50 μM.

3. Results and discussion

3.1. BLG addition induces enhancement of fluorescence of PCB

Free PCB shows emission maximum at 630 nm when excited at 580 nm (**Fig. 1A**). Incubation of BLG with PCB, at 37^{o}C during 2 hours at pH 7.2, in a dose dependent manner, induces significant enhancement of PCB fluorescence with the shift of emission maximum to 640 nm. Therefore, it seems that PCB binding to BLG causes changes in fluorescence spectra of the ligand. Significant enhancement of PCB fluorescence upon BLG addition indicates binding of pigment to protein with higher quantum yield of chromophore in bound state. It was previously shown that fluorescence of resveratrol increased upon its binding to BLG (**Liang, Tajmir-Riahi, & Subirade, 2008**). Fluorescence quantum yield of chromophore depends on rigidity of its structure. Indeed, the stretched conformation of PCB in native C-PC induces the high fluorescence in this protein, while upon denaturation chromophore has cyclic conformation and low fluorescence (**Kupka & Scheer, 2008**), suggesting that PCB in a more stretched conformation is bound to BLG.

Using equation 1, binding curve was obtained based on enhancement of PCB fluorescence upon BLG addition (**Fig. 1B**), and apparent binding constant was estimated to be $4x10^{5}$ M^{-1}. Although PCB binding to phytochrome occurs with one order of magnitude higher

binding constant (**Li, Murphy, & Lagarias, 1995**), binding of allyl isothiocyanate (AITC) to BLG has more than 10 times lower affinity in comparison to BLG-PCB system (**Keppler, Koudelka, Palani, Stuhldreier, Temps, Tholey, et al., 2014**). Therefore, PCB has moderate binding affinity for BLG.

3.2. Kinetics of BLG-PCB adduct formation

Increase of fluorescence intensity upon mixing BLG and PCB is recorded with time in order to study kinetics of pigment binding. PCB binding to BLG exhibit slows kinetics, reaching saturation after 1000 s (**Fig. 1C**). In the presence of 7 M urea binding is faster, and fluorescence intensity of BLG-PCB complex is much higher in comparison to BLG-PCB emission in buffer (**Fig. 1C**), indicating higher yield of BLG-PCB complex formation or/and higher fluorescence quantum yield of chromophore in urea. Obtained results were fitted to first order kinetics (**Fig. 1D**) and calculated apparent rate constants are 0.065 min^{-1} and 0.101 min^{-1} for reaction in the absence and presence of 7 M urea, respectively. Higher rate of BLG-PCB complex formation in 7 M urea suggests that protein unfolding did not disturb PCB binding site in protein, and that in addition to non-covalent binding covalent binding also occurs. Moreover, the fact that protein unfolding resulted in higher yield of reaction suggests that less exposed residues are targets for PCB binding. It should be mentioned that free PCB *per se* has higher fluorescence in urea (data not shown), but even with subtraction of free PCB fluorescence from adduct fluorescence, higher fluorescence of adduct in urea in comparison to its fluorescence without urea was obtained (**Fig. 1C**).

3.3. PCB covalently binds to BLG via cysteine residue

Further we aimed to examine the possibility of covalent binding of PCB to BLG. We used the ability of PCB to complex Zn^{2+} ions and form fluorescent product. SDS-PAGE of the BLG-PCB reaction mixture under non-reducing conditions, followed by Zn^{2+} staining, has showed that detected fluorescence in the gel overlaps with BLG monomer (18.4 kDa) (**Fig. 2A**). Therefore, BLG-PCB complex is preserved after SDS-PAGE, indicating formation of covalent bond between monomeric protein and the ligand. We have also recorded UV/VIS absorption spectra of the dialyzed BLG-PCB adduct. UV/VIS spectrum of free PCB (**Fig. 2B**) exhibits peaks at 330, 363 and 575 nm: peaks at 330 nm and 570 nm arise from oxidation products of pigment (**Bhat & Madyastha, 2001**) formed during 48 hours long storage. Dialyzed BLG-PCB adduct has similar UV/VIS spectra with three peaks, at 330 nm, slightly red shifted peak at 375 nm, and slightly blue shifted peak at 570 nm (**Fig. 2B**), additionally confirming covalent modification of BLG. SDS-PAGE of PCB-BLG reaction mixture in 7 M urea demonstrated higher band intensity in comparison to reaction without urea, confirming higher yield of reaction due to protein unfolding in urea (**Fig. 2C**). While incubation of free BLG in urea makes free SH groups more exposed, inducing substantial disulfide dimer formation, addition of PCB decreased band intensity arising from BLG dimer, suggesting that free cysteine residues could be involved in PCB binding (**Fig. 2C**). Moreover, fluorescence staining proves that only monomeric BLG is covalently bound to the ligand (**Fig. 2C**).

PCB is bound *via* ethylidene group to cysteine residues in phycobiliproteins (**Scheer & Zhao, 2008**). Indeed, modification of cysteine residue of BLG with IAA, followed by SDS-PAGE, has revealed that formation of fluorescent adduct is inhibited by blocking of SH group (**Fig. 3A**), further indicating binding of PCB to free cysteine residue of BLG. BLG modified with IAA in urea induced negligible rise of PCB fluorescence during time (**Fig. 3B**). Additional

confirmation of free cysteine residue of BLG involvement in covalent binding of PCB was obtained by recording fluorescent spectra of PCB incubated with free amino acids with nucleophile side chains (cysteine, lysine, arginine and histidine). Fluorescent spectrum of PCB adduct with free cysteine is similar to the spectrum of BLG-PCB adduct (**Fig. 3C**). Furthermore, fluorescent spectrum of dialyzed BLG-PCB (peak at 639 nm) is similar to the spectrum of native C-PC (peak at 642 nm) (Fig. 3D). C-PC has covalently bound PCB to Cys residues and cysteine is able to form covalent adduct with PCB (**Bishop et al., 1991**). Moreover, similarly to our results, formation of C-PC is followed by significant increase of PCB fluorescence upon addition of phycobiliprotein lyase and apo-phycocyanin (**Zhao, Wu, Zhang, Zhou, Bohm, Bubenzer, et al., 2006**). Therefore, it is obvious that PCB binds to BLG covalently *via* free cysteine residue.

Free cysteine residue of BLG is buried in the center of protein structure, making it less reactive at native conditions (**Le Maux, et al., 2014; Vetri & Militello, 2005**). Indeed, binding of PCB to BLG at pH 7.2 exhibits slow kinetics (in tens of minutes), while adduct formation obeyed pseudo-first order kinetics. Similar findings were previously described for reaction between bilins (including PCB) and apo-phytochrome (**Li, et al., 1995**). This study has proposed that holo-phytochrome formation includes two steps: the rapid, binding step with the non-covalent complex formation, followed by slow formation of thioether bond. Moreover, similar mechanism is proposed for the spontaneous attachment of PCB to apo-phycocyanin (**Arciero, Dallas, & Glazer, 1988**). Therefore, it seems that fast formation of non-covalent BLG-PCB complex precedes the slow covalent binding. In urea, unfolding of protein makes free SH group more exposed for reaction with the pigment resulting in higher yield of reaction. However, spontaneous attachment of PCB to Cys residue does not give high yield, probably due to chromophore instability (**Arciero, et al, 1988**), also noticed in the UV/VIS absorption spectra

(**Fig. 2B**). For the further experiments we have enriched BLG solution with successive addition of fresh PCB solution in order to obtain higher yield of reaction. Two substantially different assays were performed for quantification of yield of BLG-PCB adduct formation. Based on the Ellman assay, yield of adduct formation was estimated at 72 ± 1%, while quantification based on digestion of the standard protein (**Minic, et al., 2016**) estimated yield was 71 ± 6%. Therefore, these two methods gave similar results and adduct was obtained at reasonable yields to enable further characterization work.

3.4. Mass spectrometry spectra of BLG-PCB adduct

MS spectra of BLG-PCB reaction mixture is presented in **Fig. 4A**. In addition to unmodified BLG isoforms A and B, corresponding covalent adducts could be observed in all charges, suggesting that both isoforms are modified to a similar extent. MS2 spectra of ions with m/z 1335.90 (z=14), 1438.60 (z=13) and 1558.50 (z=12) demonstrate that their fragmentation results in ions with m/z the same as unmodified BLG isoform B (Figs. S3, S4A, S4B and S4C), confirming that these ions are BLG adducts. Mass increase was found to be 325 Da (Table S1), indicating that recorded adduct contains only two pyrolles bound, probably due to oxidation and fragmentation of PCB at central methylene bridge. The proposed structure similar to propentdyopents, oxidized metabolites of bilirubin (**Kunikata, Itoh, Ozaki, Kondo, Isobe, & Onishi, 2000**), is shown in **Fig. 4B**. As proposed adduct is insufficiently conjugated to absorb at about 600 nm, we believe that during applied conditions for heated electrospray ionization prior to MS analysis adduct was degraded, in line with previous observations that spontaneous attachment of PCB to apo-PC gives products with low and variable yields due to chromophore instability and propensity to oxidation (**Arciero, et al., 1988**).

3.5. PCB binding influences secondary and tertiary structure of BLG, and conformation of PCB is also changed upon binding

In order to estimate effects of PCB binding on secondary and tertiary structure of BLG, far-UV and near-UV CD spectra of dialyzed BLG-PCB adduct and free BLG were recorded. Far-UV CD spectra of unmodified BLG has negative, broad band with peak at 215 nm, due to high abundance of β-sheet secondary structure in protein (**Fig. 5A**). PCB binding induced a slight increase in negative band intensity, while the intensity of the positive band was significantly decreased in BLG-PCB adduct (Fig. 5A). Based on the obtained spectra, it was shown that free BLG contains 10% of α-helixes, 37% β-sheets, 22% β-turns and 30% of random coils. PCB binding resulted in a discrete increase of α-helical content to 12%, while content of β-sheets is decreased to 35%. Changes of β-turns (22%) and random coils (31%) contents were negligible. Similar trend was obtained in study dealing with the covalent binding of AITC to free cysteine residue of BLG (**Rade-Kukic, Schmitt, & Rawel, 2011**).

Near-UV spectrum of BLG has two characteristic peaks, at 285 and 293 nm, arising from tryptophan residues. The first one is buried in the interior of protein (Trp19), while the second one is exposed to solvent (Trp61), although some studies imply that Trp19 is mainly responsible for BLG signals in near-UV CD spectra (**Wang, Allen, & Swaisgood, 1997**). In the spectrum of BLG-PCB adduct, the peak at 285 nm becomes much more pronounced with a higher intensity, while the band intensity at the 293 nm decreases in comparison to free protein (**Fig. 5B**). Therefore, shape and amplitude of spectra indicate that tertiary structure of BLG is slightly loosened upon binding of PCB. Interestingly, Cys121 is in proximity to Trp19 residue, suggesting that PCB binding for Cys121 probably induced change in the environment of the tryptophan residue, causing changes in the near-UV CD spectrum of BLG.

Near-UV/VIS CD spectra were also recorded between 300 and 750 nm to get an insight into conformational changes of PCB upon binding to BLG (**Fig. 5C**). Free PCB has low ellipticity and poorly pronounced peaks, whilst the spectrum of the BLG-PCB complex has two bands: positive at 680 nm and negative at 380 nm, demonstrating positive Cotton effect. Therefore, PCB binding to BLG induces optical activity in tetrapyrrole chromophore through PCB conformational changes. This observation points to the conclusion that BLG binds PCB stereo-specifically. Indeed, a CD spectrum of C-PC has similar shape as BLG-PCB complex (positive VIS and negative UV band), indicating that chromophore conformation is similar in these two proteins (**Glazer, Fang, & Brown, 1973**). Moreover, study dealing with stereochemistry of PCB derivatives has shown that 3-hydro-3'-cysteinothiophycocyanobilin trimethyl ester and glutathionethiophycocyanobilin tetramethyl ester with *R* configuration at 3'C atom (3'*R*) exhibit positive Cotton effect (**Cheng & Jiang, 1992**). Therefore, it can be concluded that covalent binding of PCB to BLG induces chirality at 3'C atom with *R* configuration.

3.6. BLG-PCB adduct formation increases with increase of reaction pH

Effects of reaction's pH on adduct formation were studied by SDS-PAGE. BLG-PCB band intensities (Zn^{2+} staining) become higher with pH increase, suggesting that the yield of reaction is greater at higher pH values (pH 8 and pH 9). However, although at a lower extent, binding also occurs at low pH values (pH 2) (**Fig. S5**). Therefore, BLG has ability to covalently bind PCB over a broad pH range. Nucleophilicity of SH group strongly depends on its deprotonation, i.e. on pH value of solution (**Sardi, Manta, Portillo-Ledesma, Knoops, Comini, & Ferrer-Sueta, 2013**). At low pH, conformation of BLG is changed, probably making free cysteine residues more exposed for reaction with PCB. It was shown that Hg^{2+} could form complexes with free cysteine residue at most pH values (**Kontopidis, et al., 2004**). Therefore,

formation of BLG-PCB adduct is not only influenced by protonation state of SH group, but pH-induced conformational transitions of BLG could also influence adduct formation through change of free cysteine accessibility to PCB.

It is interesting that in both simulated gastric (pH 3) and intestinal (pH 8) fluids covalent BLG-PCB adduct is also formed (**Fig. 5D**). This implies that oral intake of PCB could result in generation of its covalent adducts with food proteins, as well as endogenous proteins of gastro-intestinal tract containing free cysteine residues.

3.7. Molecular docking reveals the binding of PCB in the calyx of BLG

We conducted a molecular docking study to determine the BLG binding sites for PCB (**Fig. 6**). One high-affinity binding site was identified showing that PCB (**Fig. 6A**) binding site is in BLG calyx (**Fig. 6B**), stabilized by hydrophobic interactions and hydrogen bonds. In this orientation, PCB molecule methylene group C3' atom is far away from thiol of single free Cys121 residue (15.35 Å) for covalent bonding (**Fig. 6C**). Furthermore, based on the inspection of all available 3D structures of BLG in PDB, Cys121 residue is overshadowed by helix and completely oriented towards protein interior away from calyx, therefore inaccessible to form covalent bond with PCB or others ligands.

It is well known that BLG is prone to disulfide exchange at higher temperatures, and the closeness of the sulfur atoms of free Cys121 and Cys106/Cys119 disulfide bond (11 Å) is compatible with intramolecular thiol/disulfide exchange reactions, resulting in release of free Cys119 (**Croguennec, Bouhallab, Molle, O'Kennedy, & Mehra, 2003**). Even after BLG incubation at 37^{o}C peptides containing both disulfides (Cys106-Cys119 and Cys106-Cys121) were identified (**Albreht, Vovk, & Simonovska, 2012**). Therefore, SMD simulation was used to simulate disulfide interchange between Cys121 and Cys119. Disulfide Cys106-Cys119 was

broken and new Cys106-Cys121 disulfide bond was created for the first 150 ns of the SMD simulation. After that, system with free Cys119 was MD simulated for further 150 ns. During the SMD simulation, there were some changes in the BLG secondary structure (especially in the β-strand containing Cys119 and Cys121) but the main 3D features of the protein (calyx and helix) remains only slightly affected (**Fig. 6D**).

A new PCB docking study, performed on the protein structure obtained after simulated disulfide interchange, showed that a PCB ligand still preferably binds to the calyx (**Fig. 6E**), but now close to the free Cys119 side-chain, as Cys119 becomes oriented towards the interior of the calyx (**Fig. 6F**). The distance between S atom from Cys119 and C3' atom from PCB ethylidene group is 5.8 Å, suggesting the possibility of covalent bond formation. Therefore, besides Cys121, Cys119 could also be the main target for reaction with PCB. In addition, chaotropes, such as urea, are known to favour BLG thiol-disulfide exchange and consequent formation of intermolecular disulfides (**Rasmussen, Barbiroli, Bonomi, Faoro, Ferranti, Iriti, et al., 2007**). Therefore, urea unfolding of protein makes free thiol groups more exposed for reaction, but also favours disulfide exchange and results in a higher extent of BLG modification, in comparison to reactions without urea in agreement with our experimental data (**Fig. 2C**).

In order to simulate covalent binding of PCB to free Cys119 after disulfide exchange, and to find the best pose of PCB in the BLG calyx, *in silico* covalent docking experiment was conducted. The covalent bond between sulfur atom from Cys119 and C3' atom from PCB induced slight changes in pigment conformation, compared to the PCB non-covalently docked to the same BLG structure (**Fig. 6G**), while PCB is still positioned in the calyx (**Fig. 6H**). Covalent attachment (**Fig. 6I**) resulted in PCB-BLG binding with high affinity, which is a consequence of additional non-covalent interactions of PCB with protein binding site residues. In the covalent

BLG-PCB adduct, PCB forms strong non-covalent hydrophobic interactions with numerous calyx residues, as well as hydrogen bonds with Val 41, Val43, Met107, Ala118 and π-π T-shaped interaction with Tyr42 (**Fig. S6**). This suggests that after disulfide interchange slightly altered calyx still exists, and it is large enough to accommodate PCB and its ethylidene C3-C3' bond in the vicinity of Cys119, while the other calyx residues interacting with PCB provide stabilization of pigment orientation favourable for covalent bond formation.

We suppose that the reaction mechanism could be based on nucleophilic addition, where thiol of Cys121 or Cys119 attacks the electrophilic ethylidene C3–C3’ bond of PCB with formation of a thioether bond, similarly to formation of thioether between BLG Cys121 and shikonin (**Albreht, et al., 2012**). According to all obtained results, we hypothesize that initially there is fast formation of non-covalent BLG-PCB complexes, with PCB binding preferentially in the calyx. In this position, free Cys121 is not properly oriented for covalent bond formation. After slight BLG conformational changes and thiol/disulfide exchange, the free thiol of Cys119 progressively becomes accessible, resulting in slow covalent binding. Our experimental results unambiguously demonstrate covalent binding, free cysteine involvement and conformational change. SMD simulation of the binding after simulated disulfide exchange in BLG supports the proposed mechanism and slightly favours Cys119 for covalent bond formation.

4. Conclusions

In this study we have examined the binding of bioactive PCB from the dietary supplement *Spirulina* to BLG, the major whey protein, using spectroscopic, electrophoretic and computational methods. Based on the results of pigment fluorescence enhancement study, slow binding kinetics and moderate binding affinity were observed. SDS-PAGE and MS of BLG-PCB

complex have revealed covalent binding of tetrapyrrole chromophore to protein, while unfolded protein has shown higher propensity to bind pigment. Blocking a free cysteine strongly inhibits BLG-PCB adduct formation, confirming involvement of this residue in PCB binding. Fluorescence and CD spectroscopy have shown changes in PCB conformation, with protein conformation slightly changed upon chromophore binding. Simulation of disulfide exchange by SMD, in combination with the docking study, demonstrated that PCB binds to BLG calyx before and after disulfide exchange, and that liberated Cys119 could also be a target for covalent bond formation due to disulfide exchange. Covalent docking study has shown that pigment covalently bound to Cys119 residue is still positioned inside the calyx of protein and forms additional non-covalent interactions with calyx residues, resulting in further stabilization of covalent BLG-PCB adduct.

The results of this study suggest that obtained covalent adduct of BLG and fluorescent pigment of microalgae can serve as a suitable delivery system of bioactive PCB. Therefore, propensity toward covalent binding of PCB makes BLG an efficient vehicle for food fortification with PCB. Indeed, spontaneous formation of covalent adduct in the conditions of the gastrointestinal tract was demonstrated in our study.

Taking into account that BLG is the major whey protein with one free SH group (Cys121), whose reactivity significantly influences techno-functional properties of this protein (**Le Maux, et al., 2014**; **Visschers & de Jongh, 2005**), and that protein structure in BLG-PCB adduct is mainly preserved, further studies are needed to reveal functional and eventual bioactive properties of this adduct.

Conflict of interest

The authors declare no conflict of interest.

Acknowledgments

The Ministry of Education, Science and Technological Development of the Republic of Serbia (Grant Number 172024) and FP7 RegPot project FCUB ERA GA No. 256716 supported this work. The EC does not share responsibility for the content of the article.

References

Albreht, A., Vovk, I., & Simonovska, B. (2012). Addition of beta-lactoglobulin produces water-soluble shikonin. *Journal of Agricultural and Food Chemistry, 60*(43), 10834-10843.

Arciero, D. M., Dallas, J. L., & Glazer, A. N. (1988). In vitro attachment of bilins to apophycocyanin. II. Determination of the structures of tryptic bilin peptides derived from the phycocyanobilin adduct. *Journal of Biological Chemistry, 263*(34), 18350-18357.

Bhat, V. B., & Madyastha, K. M. (2001). Scavenging of peroxynitrite by phycocyanin and phycocyanobilin from Spirulina platensis: protection against oxidative damage to DNA. *Biochemical and Biophysical Research Communication, 285*(2), 262-266.

Bishop, J. E., Nagy, J., O'Connell, J. F., & Rapport, H. (1991). Diastereoselective Synthesis of Phycocyanobilin-Cysteine Adducts. *Journal of American Chemical Society, 113*(21), 8024-8034.

Celej, M. S., Montich, G. G., & Fidelio, G. D. (2003). Protein stability induced by ligand binding correlates with changes in protein flexibility. *Protein Science, 12*(7), 1496-1506.

Cervantes-Llanos, M., Lagumersindez-Denis, N., Marin-Prida, J., Pavon-Fuentes, N., Falcon-Cama, V., Piniella-Matamoros, B., Camacho-Rodriguez, H., Fernandez-Masso, J. R.,

Valenzuela-Silva, C., Raices-Cruz, I., Penton-Arias, E., Teixeira, M. M., & Penton-Rol, G. (2018). Beneficial effects of oral administration of C-Phycocyanin and Phycocyanobilin in rodent models of experimental autoimmune encephalomyelitis. *Life Sciences*, *194*, 130-138.

Cheng, L., & Jiang, L. (1992). Circular dichroism and stereochemistry of the phycobilins and their derivatives. *Journal of Photochemistry and Photobiology B: Biology, 15*, 343-353.

Collini, M., D'Alfonso, L., & Baldini, G. (2000). New insight on beta-lactoglobulin binding sites by 1-anilinonaphthalene-8-sulfonate fluorescence decay. *Protein Science, 9*(10), 1968-1974.

Creamer, L. K., Bienvenue, A., Nilsson, H., Paulsson, M., van Wanroij, M., Lowe, E. K., Anema, S. G., Boland, M. J., & Jimenez-Flores, R. (2004). Heat-induced redistribution of disulfide bonds in milk proteins. 1. Bovine beta-lactoglobulin. *Journal of Agricultural and Food Chemistry*, *52*(25), 7660-7668.

Croguennec, T., Bouhallab, S., Molle, D., O'Kennedy, B. T., & Mehra, R. (2003). Stable monomeric intermediate with exposed Cys-119 is formed during heat denaturation of beta-lactoglobulin. *Biochemical and Biophysical Research Communication, 301*(2), 465-471.

Ellman, G., & Lysko, H. (1979). A precise method for the determination of whole blood and plasma sulfhydryl groups. *Analytical Biochemistry*, *93*(1), 98-102.

Fernández-Rojas, B., Hernández-Juárez, J., & Pedraza-Chaverri, J. (2014). Nutraceutical properties of phycocyanin. *Journal of Functional Foods, 11*, 375-392.

Glazer, A. N., Fang, S., & Brown, D. M. (1973). Spectroscopic properties of C-phycocyanin and of its alpha and beta subunits. *Journal of Biological Chemistry*, *248*(16), 5679-5685.

Gottschalk, M., Nilsson, H., Roos, H., & Halle, B. (2003). Protein self-association in solution: the bovine beta -lactoglobulin dimer and octamer. *Protein Science, 12*(11), 2404-2411.

Jespersen, L., Stromdahl, L. D., Olsen, K., & Skibsted, L. H. (2005). Heat and light stability of three natural blue colorants for use in confectionery and beverages. *European Food Research and Technology, 220*(3-4), 261-266.

Keppler, J. K., Koudelka, T., Palani, K., Stuhldreier, M. C., Temps, F., Tholey, A., & Schwarz, K. (2014). Characterization of the covalent binding of allyl isothiocyanate to beta-lactoglobulin by fluorescence quenching, equilibrium measurement, and mass spectrometry. *Journal of Biomolecular Structure and Dynamics, 32*(7), 1103-1117.

Keppler, J. K., Stuhldreier, M. C., Temps, F., & Schwarz, K. (2014). Influence of mathematical models and correction factors on binding results of polyphenols and retinol with β-lactoglobulin measured with fluorescence quenching. *Food Biophysics, 9*(2), 158-168.

Klein, G., & Rüdiger, W. (1979). Thioether Formation of Phycocyanobilin: A Model Reaction of Phycocyanin Biosynthesis. *Zeitschrift für Naturforschung, 34c*, 192-195.

Kontopidis, G., Holt, C., & Sawyer, L. (2004). Invited review: beta-lactoglobulin: binding properties, structure, and function. *Journal of Dairy Science, 87*(4), 785-796.

Kunikata, T., Itoh, S., Ozaki, T., Kondo, M., Isobe, K., & Onishi, S. (2000). Formation of propentdyopents and biliverdin, oxidized metabolites of bilirubin, in infants receiving oxygen therapy. *Pediatrics International, 42*(4), 331-336.

Kupka, M., & Scheer, H. (2008). Unfolding of C-phycocyanin followed by loss of non-covalent chromophore-protein interactions 1. Equilibrium experiments. *Biochimica et Biophysica Acta, 1777*(1), 94-103.

Le Maux, S., Bouhallab, S., Giblin, L., Brodkorb, A., & Croguennec, T. (2014). Bovine beta-lactoglobulin/fatty acid complexes: binding, structural, and biological properties. *Dairy Science and Technology, 94*, 409-426.

Li, L., Murphy, J. T., & Lagarias, J. C. (1995). Continuous fluorescence assay of phytochrome assembly in vitro. *Biochemistry, 34*(24), 7923-7930.

Liang, L., Tajmir-Riahi, H. A., & Subirade, M. (2008). Interaction of beta-lactoglobulin with resveratrol and its biological implications. *Biomacromolecules, 9*(1), 50-56.

Minekus, M., Alminger, M., Alvito, P., Ballance, S., Bohn, T., Bourlieu, C., Carriere, F., Boutrou, R., Corredig, M., Dupont, D., Dufour, C., Egger, L., Golding, M., Karakaya, S., Kirkhus, B., Le Feunteun, S., Lesmes, U., Macierzanka, A., Mackie, A., Marze, S., McClements, D. J., Menard, O., Recio, I., Santos, C. N., Singh, R. P., Vegarud, G. E., Wickham, M. S., Weitschies, W., & Brodkorb, A. (2014). A standardised static in vitro digestion method suitable for food - an international consensus. *Food and Function, 5*(6), 1113-1124.

Minic, S., Stanic-Vucinic, D., Radomirovic, M., Radibratovic, M., Milcic, M., Nikolic, M., & Cirkovic Velickovic, T. (2018). Characterization and effects of binding of food-derived bioactive phycocyanobilin to bovine serum albumin. *Food Chemistry, 239*, 1090-1099.

Minic, S. L., Milcic, M., Stanic-Vucinic, D., Radibratovic, M., Sotiroudis, T. G., Nikolic, M. R., & Velickovic, T. Ć. (2015). Phycocyanobilin, a bioactive tetrapyrrolic compound of blue-green alga Spirulina, binds with high affinity and competes with bilirubin for binding on human serum albumin. *RSC Advances, 5*(76), 61787-61798.

Minic, S. L., Stanic-Vucinic, D., Mihailovic, J., Krstic, M., Nikolic, M. R., & Cirkovic Velickovic, T. (2016). Digestion by pepsin releases biologically active chromopeptides

from C-phycocyanin, a blue-colored biliprotein of microalga Spirulina. *Journal of Proteomics, 147,* 132-139.

Mysliwa-Kurdziel, B., & Solymosi, K. (2017). Phycobilins and Phycobiliproteins Used in Food Industry and Medicine. *Mini-Reviews in Medicinal Chemistry, 17*(13), 1173-1193.

Penton-Rol, G., Marin-Prida, J., & Falcon-Cama, V. (2018). C-Phycocyanin and Phycocyanobilin as Remyelination Therapies for Enhancing Recovery in Multiple Sclerosis and Ischemic Stroke: A Preclinical Perspective. *Behavioral Sciences (Basel), 8*(1), pii: E15.

Rade-Kukic, K., Schmitt, C., & Rawel, H. M. (2011). Formation of conjugates between β-lactoglobulin and allyl isothiocyanate: Effect on protein heat aggregation, foaming and emulsifying properties. *Food Hydrocolloids, 25*(4), 694-706.

Radibratovic, M., Minic, S., Stanic-Vucinic, D., Nikolic, M., Milcic, M., & Cirkovic Velickovic, T. (2016). Stabilization of Human Serum Albumin by the Binding of Phycocyanobilin, a Bioactive Chromophore of Blue-Green Alga Spirulina: Molecular Dynamics and Experimental Study. *PLoS One, 11*(12), e0167973.

Rasmussen, P., Barbiroli, A., Bonomi, F., Faoro, F., Ferranti, P., Iriti, M., Picariello, G., & Iametti, S. (2007). Formation of structured polymers upon controlled denaturation of beta-lactoglobulin with different chaotropes. *Biopolymers, 86*(1), 57-72.

Sardi, F., Manta, B., Portillo-Ledesma, S., Knoops, B., Comini, M. A., & Ferrer-Sueta, G. (2013). Determination of acidity and nucleophilicity in thiols by reaction with monobromobimane and fluorescence detection. *Analytical Biochemistry, 435*(1), 74-82.

Scheer, H., & Zhao, K. H. (2008). Biliprotein maturation: the chromophore attachment. *Molecular Microbiology, 68*(2), 263-276.

Singh, H. (2011). Aspects of milk-protein-stabilised emulsions. *Food Hydrocolloids*, *25*(8), 1938-1944.

Stojadinovic, M., Burazer, L., Ercili-Cura, D., Sancho, A., Buchert, J., Cirkovic Velickovic, T., & Stanic-Vucinic, D. (2012). One-step method for isolation and purification of native beta-lactoglobulin from bovine whey. *Journal of the Science of Food and Agriculture*, *92*(7), 1432-1440.

Teng, Z., Xu, R., & Wang, Q. (2015). Beta-lactoglobulin-based encapsulating systems as emerging bioavailability enhancers for nutraceuticals: a review. *RSC Advances*, *5*(44), 35138-35154.

Vetri, V., & Militello, V. (2005). Thermal induced conformational changes involved in the aggregation pathways of beta-lactoglobulin. *Biophysical Chemistry*, *113*(1), 83-91.

Visschers, R. W., & de Jongh, H. H. (2005). Disulphide bond formation in food protein aggregation and gelation. *Biotechnology Advances*, *23*(1), 75-80.

Wang, Q., Allen, J. C., & Swaisgood, H. E. (1997). Binding of retinoids to beta-lactoglobulin isolated by bioselective adsorption. *Journal of Dairy Science*, *80*(6), 1047-1053.

Zhang, Y.-M., & Chen, F. (1999). A simple method for efficient separation and purification of C-phycocyanin and allophycocyanin from Spirulina platensis. *Biotechnology Techniques*, *13*, 601-603.

Zhao, K. H., Wu, D., Zhang, L., Zhou, M., Bohm, S., Bubenzer, C., & Scheer, H. (2006). Chromophore attachment in phycocyanin. Functional amino acids of phycocyanobilin alpha-phycocyanin lyase and evidence for chromophore binding. *The FEBS Journal*, *273*(6), 1262-1274.

Zhou, Z.-P., Liu, L.-N., Chen, X.-L., Wang, J.-X., Chen, M., Zhang, Y.-Z., & Zhou, B.-C. (2005). Factors that effect antioxidant activity of C-phycocyanin from Spirulina platensis. *Journal of Food Biochemistry, 29*, 313-322.

Figure Captions:

Figure 1. (**A**) Emission spectra of PCB in the absence and in the presence of different concentrations of BLG (excitation at 580 nm); (**B**) Binding curve plot of BLG-induced enhancement of PCB fluorescence; (**C**) Kinetics of BLG-PCB adduct formation in the absence and in the presence of 7 M urea, studied by increase of PCB fluorescence upon BLG addition (excitation at 580 nm); (**D**) Fitting of the free PCB concentration change during time into first order kinetics.

Figure 2. (**A**) SDS-PAGE (16% PAA gel, non-reducing conditions) of free BLG (1), free PCB (2), and BLG-PCB complex (3). Left: CBB staining; Right: Zn^{2+} staining; (**B**) UV/VIS absorption spectra of dialyzed BLG-PCB complex, free BLG and free PCB; (**C**) SDS-PAGE (16% PAA gel, non-reducing conditions) of free PCB, free BLG and BLG-PCB complex in the absence (1, 3, 5; respectively) and in the presence of 7 M urea (2, 4, 6; respectively). Left: Zn^{2+} staining; right: CBB staining.

Figure 3. (**A**) Inhibition of PCB binding to BLG by IAA (SDS-PAGE, 16% PAA gel, non-reducing conditions): 1) 20 μM BLG; 2) 20 μM PCB; 3) BLG:PCB (20 μM both); 4) BLG:PCB (20 μM both) + 20 μM IAA; 5) BLG:PCB (20 μM both) + 200 μM IAA; 6) BLG:PCB (20 μM both) + 2 mM IAA; 7) 20 μM BLG + 20 mM IAA; 8) 20 μM BLG + 200 μM IAA; 9) 20 μM BLG + 2 mM IAA. Left: CBB staining; right: Zn^{2+} staining; (**B**) Effects of free cysteine residue

modification by IAA on kinetics of BLG-PCB adduct formation (in the presence of 7 M urea); (**C**) Emission spectra of PCB (excitation at 580 nm) in the absence and in the presence of BLG and amino acids; (**D**) Emission spectra of dialyzed BLG-PCB adduct and native C-PC (excitation at 580 nm).

Figure 4. (**A**) MS spectrum of 20 μM BLG incubated in the presence of 20 μM PCB for 2 hours at 37^{o}C in 20 mM phosphate buffer pH 7.2; (**B**) Proposed structure of covalent adduct of BLG with PCB oxidation derivative after MS spectrometry.

Figure 5. (**A**) Far-UV CD spectra of dialyzed BLG-PCB complex and free BLG; (**B**) Near-UV CD spectra of dialyzed BLG-PCB complex and free BLG; (**C**) Near-UV/VIS CD spectra of dialyzed BLG-PCB complex, free BLG and free PCB; (**D**) SDS-PAGE (12% PAA gel, non-reducing conditions) of free BLG after incubation with PCB in simulated gastrointestinal fluids: (1) saliva fluid, (2) saliva fluid followed by gastric fluid, and (3) saliva fluid followed by gastric fluid and then intestinal fluid. Left: CBB staining; Right: Zn^{2+} staining.

Figure 6. (**A**) Chemical structure of PCB; Molecular docking of PCB (violet) bound in calyx of BLG (PDB ID: 3NQ3) is presented as a solvent accessible surface model (B) and as the close-up view of ribbon model (**C**). Cys106, Cys119 and Cys121 residues are presented as sticks with S atoms in yellow; the distances between C3' atom of PCB and S atom of corresponding cysteine residues are labeled in black; (**D**) Superimposed 3D structures of BLG before (red) and after (green) steered molecular dynamics (SMD) simulation simulating disulfide exchange (break up of Cys106-Cys119 disulfide and creation of Cys106-Cys121 disulfide); Molecular docking of PCB (violet) bound in calyx of BLG after SMD simulation (**Fig. 6D**) is presented as a solvent accessible surface model (E) and as the close-up view of ribbon model (F); (**G**) Superimposed 3D structures of PCB bound to BLG after SMD simulation by non-covalent (violet) and covalent

(orange) docking; Covalent docking of PCB (orange) bound in calyx of BLG after SMD simulation is presented as solvent accessible surface model (**H**), and as the close-up view of ribbon model (**I**).

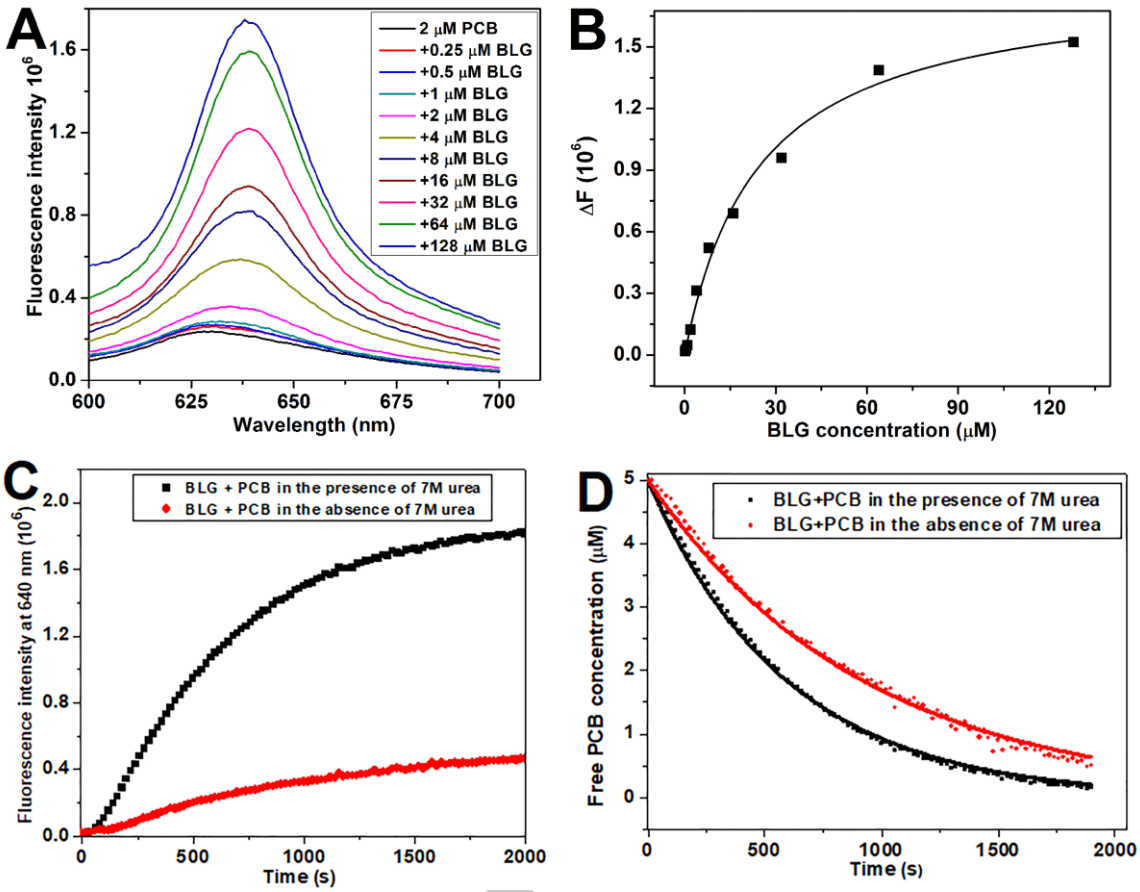

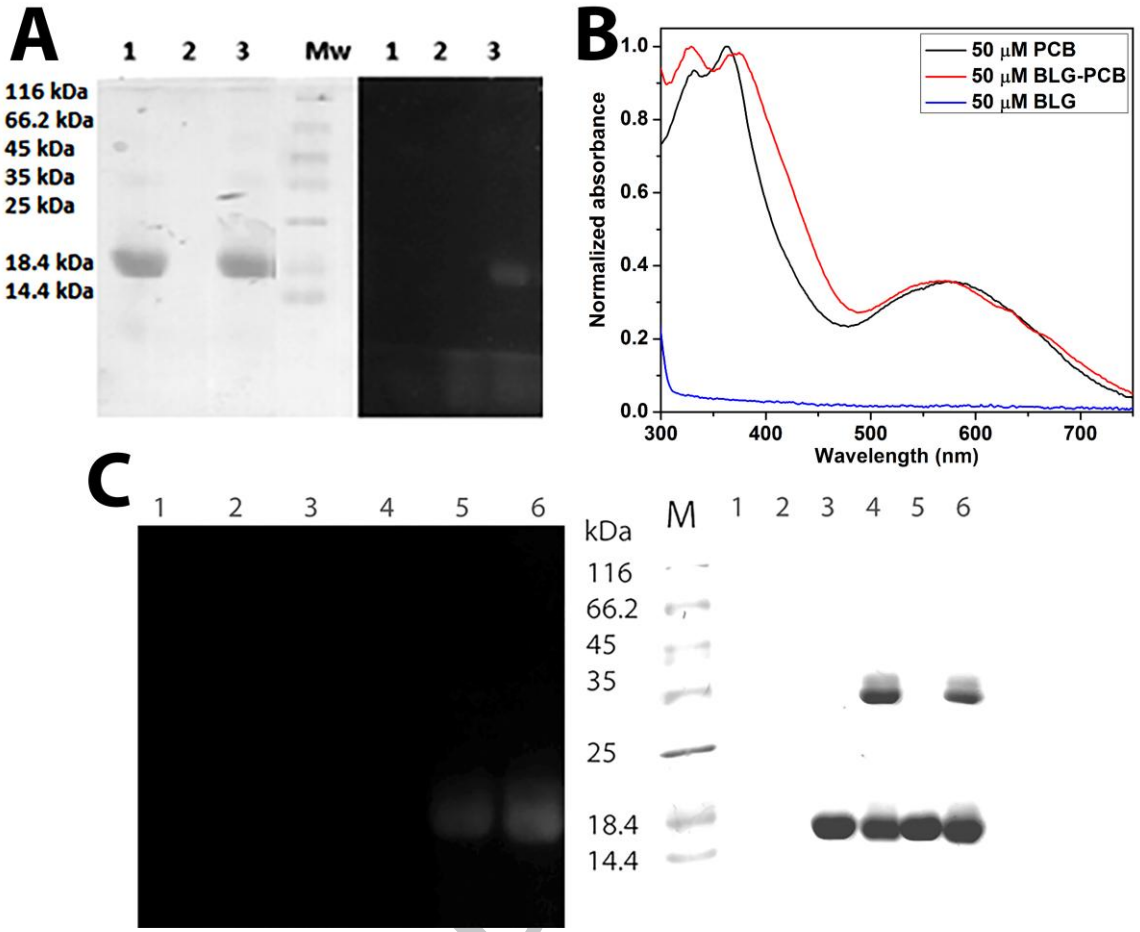
A
1 2 3 Mw 1 2 3
116 kDa
66.2 kDa
45 kDa
35 kDa
25 kDa
18.4 kDa
14.4 kDa
B
50 μM PCB
50 μM BLG-PCB
50 μM BLG
Normalized absorbance
Wavelength (nm)
C
1 2 3 4 5 6
kDa
M 1 2 3 4 5 6
116
66.2
45
35
25
18.4
14.4

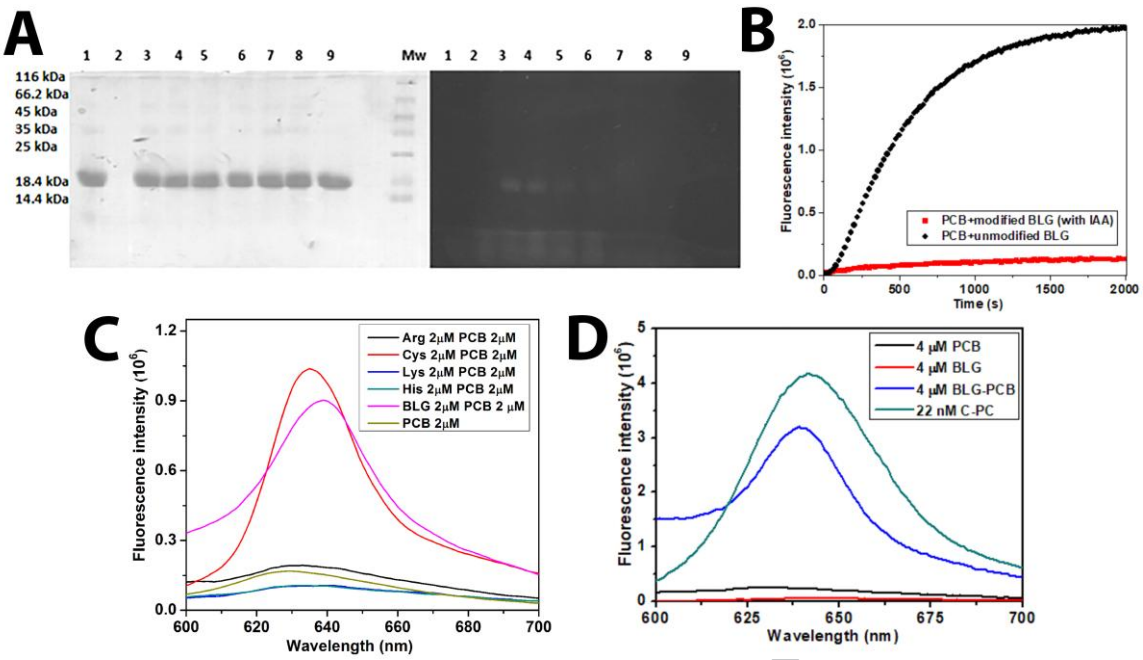

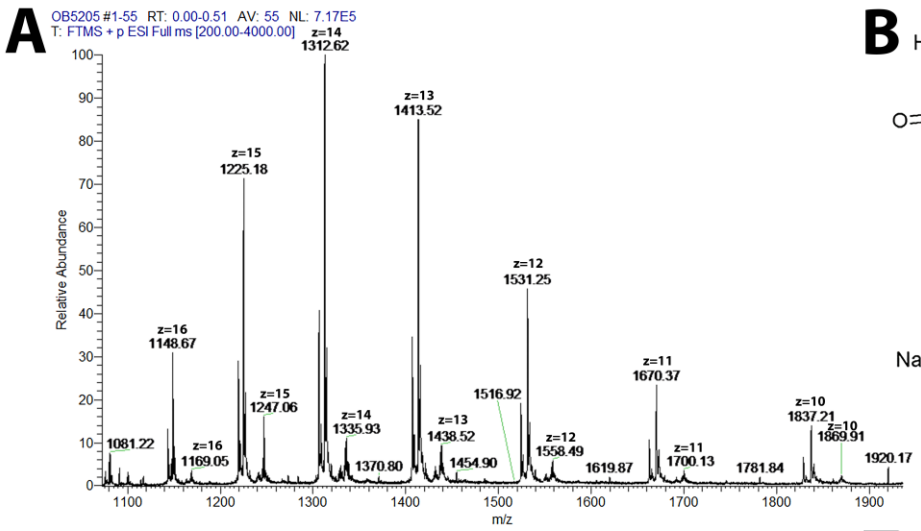

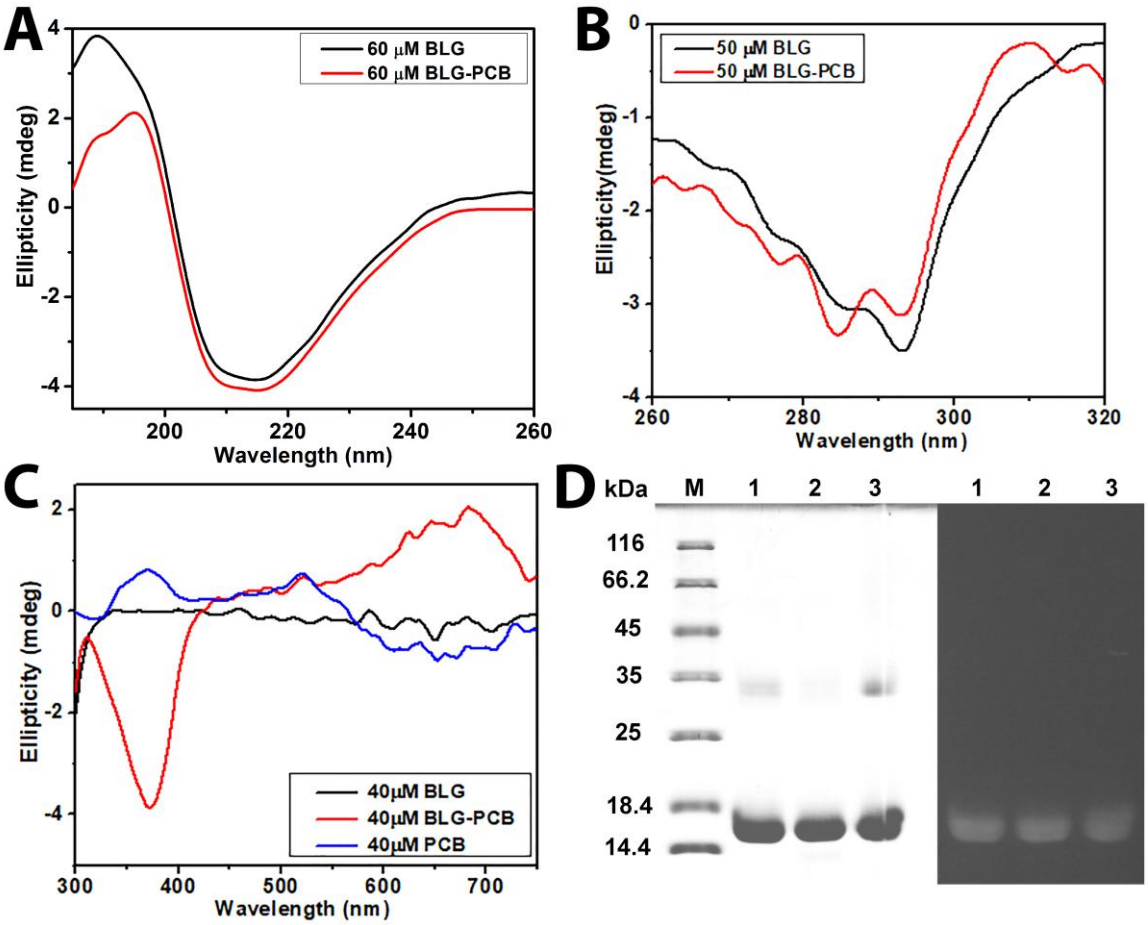

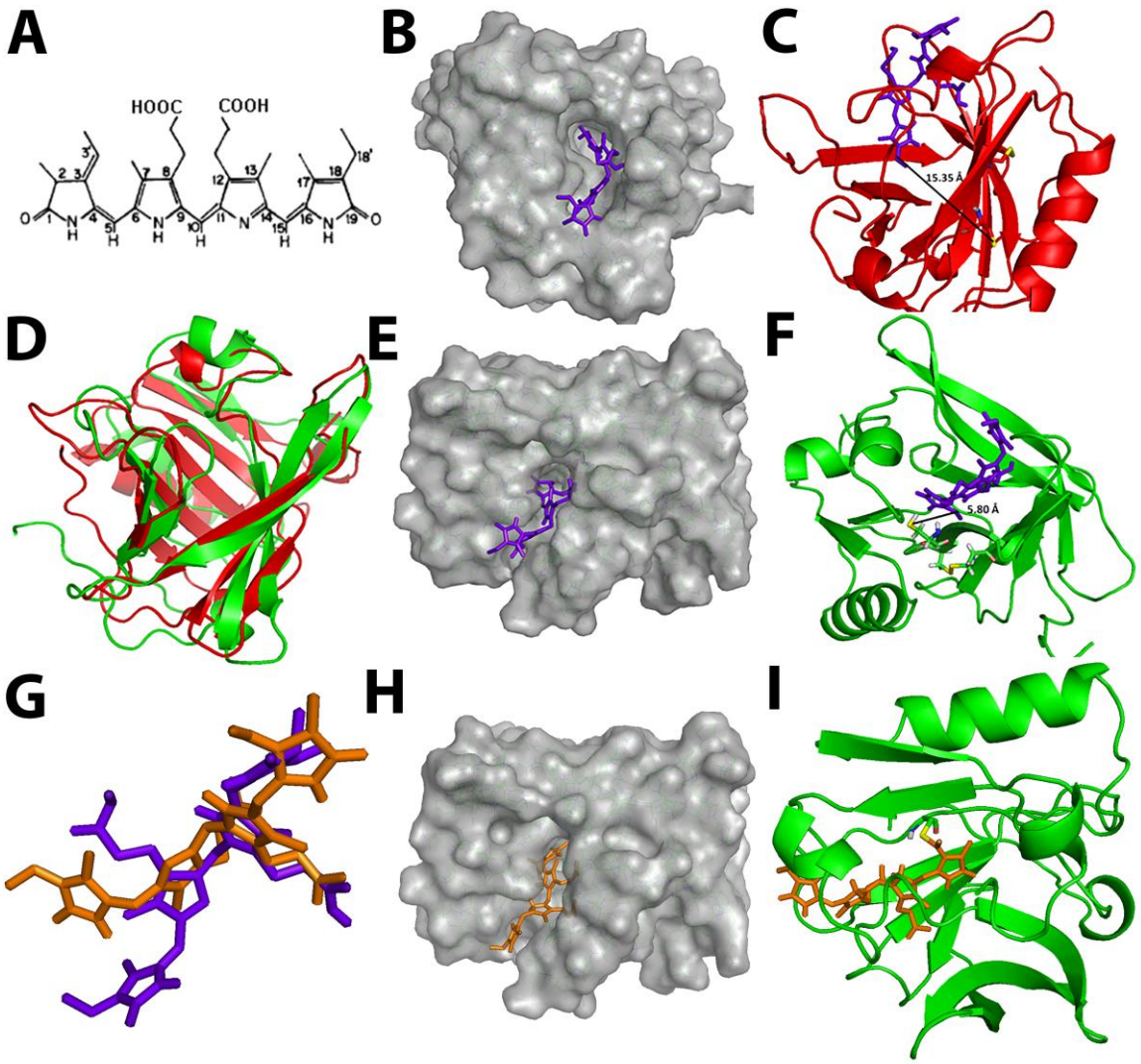

Highlights

Phycocyanobilin (PCB) binds covalently to bovine β-lactoglobulin (BLG) *via* free Cys;

Binding is slow, of moderate affinity (K_a=4 x 10^4 M^{-1}), and stereo-selective;

The adduct has slightly altered secondary and tertiary protein structure;

Binding occurs under simulated gastrointestinal conditions;

Steered molecular dynamic puts PCB in the BLG calyx in the proximity of free Cys119.